

Reaction Mechanism and Kinetics of Boron Removal from Molten Silicon by CaO–SiO₂–CaCl₂ Slag Treatment

Ye Wang¹ · Kazuki Morita¹

Published online: 1 April 2015

© The Minerals, Metals & Materials Society (TMS) 2015

Abstract The mechanism by which B is removed from Si to a molten CaO–SiO₂–CaCl₂ slag, and its subsequent evaporation to a gas phase at 1723 K, has been evaluated with a view to optimize the production of solar-grade Si. By assuming a diffusion model for the transfer of B from Si to molten slag, and its evaporation to a gas phase, the diffusion coefficient of B in slag was investigated using the tube-molten pool method. The mass transfer coefficients of B in slag were also measured and calculated according to Fick's law. Through this, it was found that the rate-limiting step of B removal in the slag refining process is controlled by B transfer from both the slag interface and surface. Of these, however, it is the former that has the greater influence, as the slag boundary layers in the interface are thicker than those at the surface.

Keywords Solar-grade silicon · Slag refining · Boron removal · Mass transfer coefficient · Diffusion coefficient

Introduction

The availability of abundant and low-cost solar-grade Si (SOG-Si) feedstock is essential to support the widespread use of solar cells; and indeed, there has been great progress in reducing energy consumption in the modified Siemens and fluidized bed reactor processes of fabricating SOG-Si.

However, the potential for cost reduction in these processes is limited by the low productivity of Si and the amount of chemical energy required to convert metallurgical-grade Si (MG-Si) into gaseous compounds, not to mention the distillation, reduction, and deposition of these compounds as solid Si. A more cost-effective and energy-efficient alternative to produce SOG-Si is to use a metallurgical process, which provides sustainability and a number of benefits in terms of productivity and process cost. Metallurgical methods such as directional solidification [1–3], alloy refining [4–6], oxidation with plasma melting [7, 8], and vacuum melting [9, 10] have all been investigated; however, each has its own unique limitations that prevent the total removal of impurities. This is largely a result of the fact that the segregation coefficients of B and P are both close to 1 in molten Si, meaning that they are not easily removed from the melt. Thus, in order to meet the strong demand for Si that is free of B and P via a low-cost process, the use of slag treatment as a method for the removal of B and P has received increased attention owing to its low cost and mass productivity.

In slag treatment, ternary slags of CaO–SiO₂–CaCl₂ have been confirmed to be effective in removing B, with a decrease in concentration from 150 to approximately 30 ppmw having been achieved at 1723 K (1450 °C) along with a B-removal efficiency as high as 86 % [11]. Though this study provides a foundation, there is clearly a need for further research into the transportation kinetics of B from molten Si to molten slag, and its evaporation from slag to a gas phase. Thus, in the present study, a model for the mass transfer of B from molten Si through slag to the gas phase is first discussed. The diffusion coefficient of B in molten Si has been previously reported [12]; however, its diffusion coefficient in molten CaO–SiO₂–CaCl₂ slag is still undefined. To address this, the diffusion coefficient of B in

✉ Ye Wang
280405702@qq.com; wangye@iis.u-tokyo.ac.jp

¹ Department of Materials Engineering, The University of Tokyo, 4-6-1 Bunkyo, Tokyo 113-8656, Japan

CaO–SiO₂–CaCl₂ slag was investigated by the tube-molten pool method at 1723 K. Finally, in order to investigate the rate controlling step and quantify the mass transfer of B from molten Si through slag to the gas phase, the mass transfer coefficients of B in the slag were also characterized.

Experimental Procedure

Measuring the Diffusion Coefficient of B

To measure the diffusion coefficient of B in molten slag, a graphite tube (length = 20 mm, width = 15 mm, height = 12 mm) was prepared with holes measuring 1.5 mm. Next, 20 g of different CaO–SiO₂–CaCl₂ slag system compositions were mixed in a graphite crucible and premelted in an induction furnace under vacuum, into which the graphite tube was immersed for 10 min. A flow of Ar gas was then introduced to force the slag into the vacuum tube, which was finally lifted up and the furnace cooled to produce a slag-filled tube.

Diffusion coefficient experiments were carried out by first melting 30 g of the same slag composition with 100 ppmw of B in a resistance furnace at 1723 K (1450 °C) for 5 min, into which the slag-filled tube was immersed for 20 min. After the tube was removed, it was cut into portions (as shown in Fig. 1), and the slag was collected from the hole. The B concentration (C_B) of each portion ($l = 2$ mm) of the tube was analyzed by inductively coupled plasma atomic emission spectrometry (ICP-AES).

Measuring the Mass Transfer Coefficient of B

The mass transfer coefficient was measured using a vertical SiC resistance furnace (60 mm O.D., 53 mm I.D., 1000 mm length), the temperature of which was maintained at 1723 ± 2 K using a PID controller (Fig. 2). For this, 3 g of Si containing 300 ppmw of B was premelted at 1723 K, and then, 3, 6, or 9 g of 30 mol %CaO–23 mol %SiO₂–47 mol %CaCl₂ slag was added and held at 1723 K under an Ar atmosphere for various periods of time. A NaOH solution was used to absorb any evaporated Cl-containing gas and after the experiment, the B concentration in the slag $[(B^{3+})_b]$ and Si $([B]_b)$ was measured by ICP-AES.

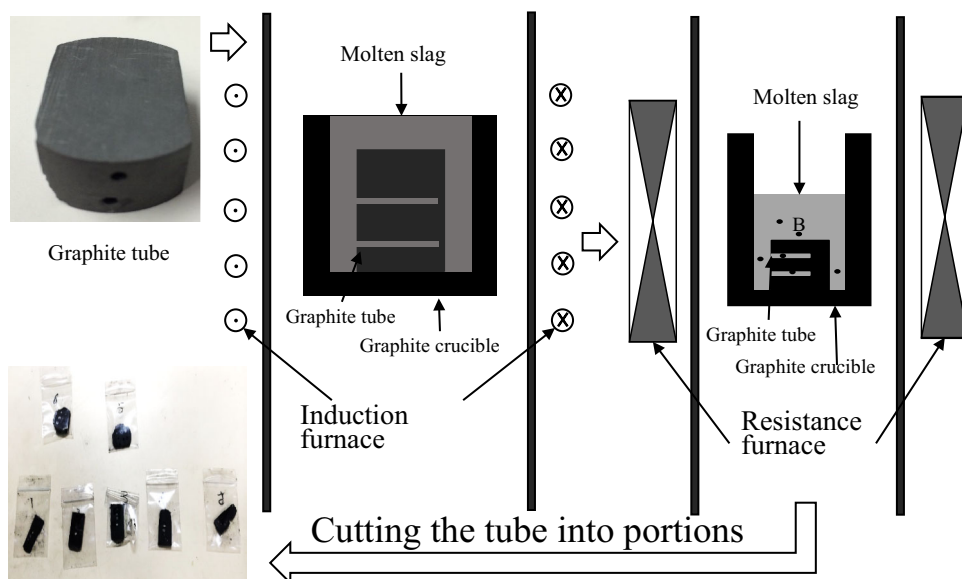
Results and Discussion

Diffusion Coefficient Measurement

Figure 3 and Table 1 show the B distributions obtained with the four different slag compositions after 20 min at 1723 K, in which it can be clearly seen that the concentration of B (C_B) decreases from 100 to 0 ppmw with increasing distance from the end of the tube (x).

If it is assumed that diffusion in the slag is dimensionally sufficiently long, then diffusion can be considered to begin at one edge of the slag, with the concentration remaining 0 at the other side. This type of diffusion can be expressed using the semi-infinite one-dimensional model, wherein the range of the diffusion distance, x , is $[0, \infty]$. At time $t = 0$, it can be expressed as follows:

Fig. 1 Schematic of diffusion coefficient experiment



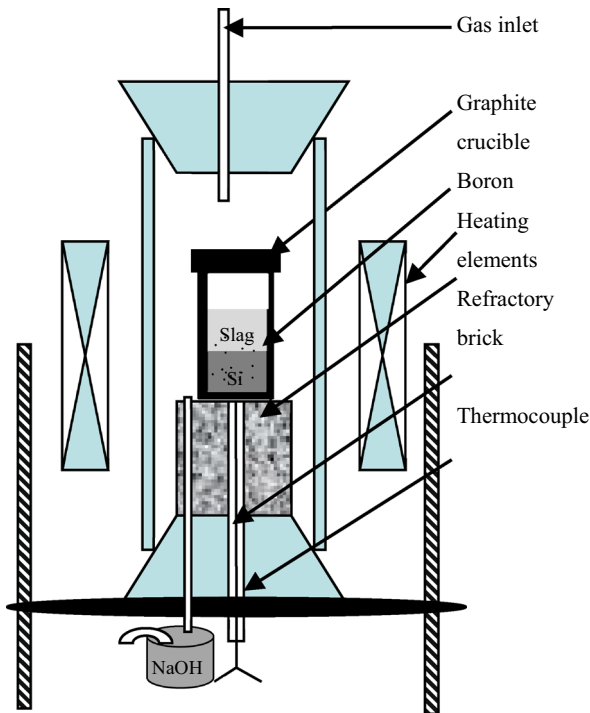


Fig. 2 Experimental set up of resistance furnace

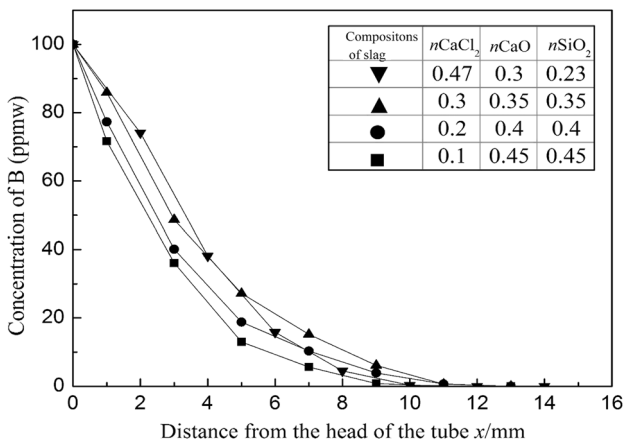


Fig. 3 Relationship between slag composition and the concentration of B at various positions

$$\frac{\partial C}{\partial t} = \frac{\partial}{\partial x} \left(D \frac{\partial C}{\partial x} \right), C_B(x, t) = C_B^0 - (C_B^0 - C_0) \operatorname{erf} \left(\frac{x}{2\sqrt{D_s t}} \right) \quad (1)$$

$$\text{Initial condition } C(x, 0) = C_0 (t = 0) \quad (2)$$

$$\text{Boundary condition} = \begin{cases} C(0, t) = C_B^0 \\ C(\infty, t) = C_0 \end{cases} (t > 0) \quad (3)$$

Here, C_B represents the concentration of B in the slag at various positions, while C_B^0 is the initial concentration at

the edge and is regarded as being equal to the concentration of the solute diffusion source (100 ppmw); C_0 is the concentration of slag in the tube, which is 0; D_s is the diffusion coefficient; and t is the diffusion time, $t = 1200$ s. $\operatorname{Erf}(y)$ is the error function.

After taking the definite integral, Eq. (1) can be expressed as

$$\frac{C_B - C_B^0}{C_0 - C_B^0} = \frac{2}{\sqrt{\pi}} \int_0^{x/(2\sqrt{D_s t})} e^{-\lambda^2} d\lambda \quad (4)$$

The right-hand side of Eq. (4) is the error function, which is $\operatorname{erf}(y)$ and $C_0 = 0$. Thus, the equation can be simplified as

$$C_B = C_B^0 \left[1 - \operatorname{erf} \left(\frac{x}{2\sqrt{D_s t}} \right) \right] \quad (5)$$

The value of D can therefore be calculated from C_B , C_B^0 , and the table of error for $\operatorname{erf}(y)$.

The diffusion coefficients obtained using Eq. (5) are shown in Fig. 4, in which the slopes of x^2 and $4y^2 t$ are the diffusion coefficients of the four different slag compositions. The accurate values of C_B and D_s are shown in Table 1.

The value of D_s was found to increase from 4.5×10^{-9} to 8.46×10^{-9} m²/s when the CaCl₂ concentration was increased from 10 to 47 mol %, as shown in Fig. 5. Given that CaCl₂ can decrease the viscosity of the slag, the maximum value shows that the solubility of CaCl₂ in a CaCl₂–CaO–SiO₂ slag is approximately 50 %.

Table 2 compares the diffusion of different elements in various slag systems, revealing that the diffusion of B in a CaO–SiO₂–CaCl₂ slag is faster than the diffusion of S in the more viscous CaO–SiO₂–Al₂O₃ slag system. Moreover, the diffusion of B is faster in molten Si than in slag, suggesting that the rate-limiting step in the B-removal process may be controlled by the transportation of B in the slag. However, the diffusion of B in slag can be separated into two distinct steps depending on whether it occurs at interface or surface of the slag. To investigate the diffusion of B in the bulk slag, its mass transfer coefficient in the slag needs to be considered.

Mass Transfer Coefficient of B in Slag

The positions within the sample used for B analysis in slag and Si were, as shown in Table 3, at the top of the slag and the bottom of the Si, as the distribution of B in both was homogeneous. The mass transfer coefficient measurements are also shown in Table 3, wherein the ratio of B removed to the gas phase was defined as $(300 - C_B \text{ in Si} - \mu \cdot C_B \text{ in slag}) / 300$; μ being the mass ratio between slag and Si ($\mu = 1, 2, 3$). It is evident from this that 40–60 % of the B is

Table 1 Diffusion coefficients and B concentrations

| Distance from the head of the tube x/mm | | 2.0 | 4.0 | 6.0 | 8.0 | 10 | 12 | 14 | D_s |
|--|--|------|------|------|------|------|------|-----|--|
| Composition of slag | C_B (ppmw) | 74.1 | 38.1 | 15.8 | 4.5 | 0.3 | 0 | 0 | $8.46 \times 10^{-9} \text{ m}^2 \text{ s}^{-1}$ |
| $x_{\text{CaCl}_2} : x_{\text{CaO}} : x_{\text{SiO}_2} = 47:30:23$ | D_B ($10^{-8} \text{ m}^2 \text{ s}^{-1}$) | 1.5 | 0.87 | 0.74 | 0.66 | 0.45 | – | – | |
| Distance from the head of the tube x/mm | | 1.0 | 3.0 | 5.0 | 7.0 | 9.0 | 11 | 13 | D_s |
| Composition of slag | C_B (ppmw) | 85.9 | 48.7 | 27.2 | 15.2 | 6.1 | 0.6 | 0.0 | $8.41 \times 10^{-9} \text{ m}^2 \text{ s}^{-1}$ |
| $x_{\text{CaCl}_2} : x_{\text{CaO}} : x_{\text{SiO}_2} = 30:35:35$ | D_B ($10^{-8} \text{ m}^2 \text{ s}^{-1}$) | 1.3 | 0.75 | 0.86 | 0.98 | 0.95 | 0.66 | – | |
| Composition of slag | C_B (ppmw) | 77.3 | 40.1 | 18.8 | 10.3 | 3.9 | 0.7 | 0.0 | $6.50 \times 10^{-9} \text{ m}^2 \text{ s}^{-1}$ |
| $x_{\text{CaCl}_2} : x_{\text{CaO}} : x_{\text{SiO}_2} = 20:40:40$ | D_B ($10^{-8} \text{ m}^2 \text{ s}^{-1}$) | 0.52 | 0.52 | 0.60 | 0.77 | 0.79 | 0.69 | – | |
| Composition of slag | C_B (ppmw) | 71.6 | 36.1 | 13.0 | 5.6 | 0.8 | 0.0 | 0.0 | $4.50 \times 10^{-9} \text{ m}^2 \text{ s}^{-1}$ |
| $x_{\text{CaCl}_2} : x_{\text{CaO}} : x_{\text{SiO}_2} = 10:45:45$ | D_B ($10^{-8} \text{ m}^2 \text{ s}^{-1}$) | 0.31 | 0.46 | 0.45 | 0.56 | 0 | – | – | |

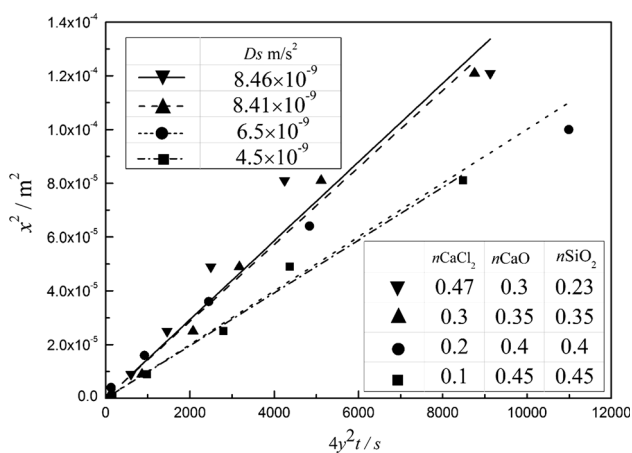


Fig. 4 Diffusion coefficients of four different slags

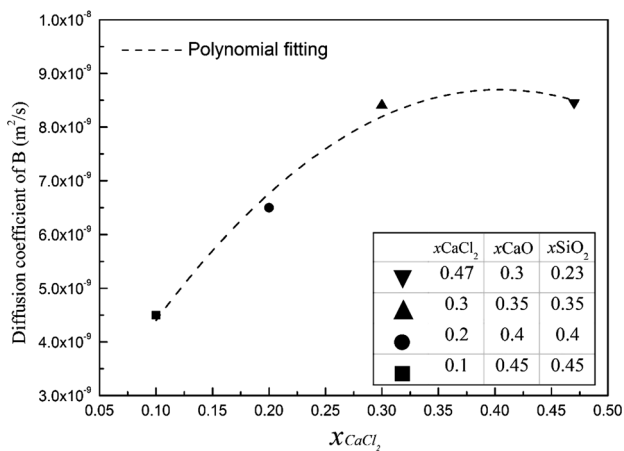


Fig. 5 Change in the diffusion coefficient of B with slag composition

evaporated as gas phase. Moreover, from the mass ratios between Si and slag, we see that the B concentration in the molten Si decreased from 300 to approximately 30 ppmw, while the concentration in the slag increased from 0 to

approximately 40 ppmw, after 3600 s at 1723 K. The mass transfer coefficient of B in the slag boundary layer adjacent to Si (k_i) and the surface (k_s) will be discussed in the next section.

Kinetics of B Removal Using a CaO–SiO₂–CaCl₂ Slag

The process of removing B using a CaO–SiO₂–CaCl₂ slag can be divided into six steps (1) mass transport in Si, (2) chemical reaction at the interface between the slag and Si, (3) mass transport in the slag from the interface to the bulk, (4) mass transport from the bulk to the surface, (5) chemical reaction at the surface, and finally, (6) evaporation from surface to the gas phase.

In Fig. 6, $[B]_i$, $[B]_b$, $(B^{3+})_i$, $(B^{3+})_b$, and $\{B^{3+}\}_s$ represent the weight concentration of B in: the molten Si interface, the bulk molten Si, the interface between Si and slag, the molten slag bulk, and the surface of the molten slag. The variables $C_{B_i^{3+}}$ and $C_{B_b^{3+}}$ are the mole concentrations of B in the interface and bulk of the slag phase, respectively, while J_i is the mass flux of B in step i ($i = 1-6$). Assuming that the concentration of B in the bulk slag is homogeneous because of convection but changes over time in the boundary layer at the interface and surface, C_B can be considered a function of t in the boundary layers and the process can be simplified to one of unsteady-state diffusion.

In order to confirm the homogeneity of B in the slag and Si phases, the slag and Si of sample I-2 was analyzed at various points by ICP. As shown in Fig. 7, this revealed that the B content of the slag was consistently approximately 20.7 ppmw, whereas that of the Si was much higher at approximately 233.5 ppmw. As each value represents an average of three readings, this demonstrates that the distribution of B in both phases was indeed homogeneous.

Table 2 Diffusion coefficients of different series

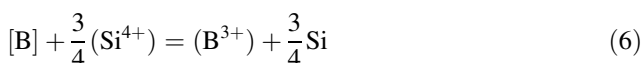
| Diffusant | Material system (mass %) | D (m ² /s) | T (K) |
|-----------|---|--------------------------------|------------|
| B | CaO–SiO ₂ –CaCl ₂ (0.15–0.18–0.66) | 8.46×10^{-9} | 1723 |
| S [13] | CaO–SiO ₂ –Al ₂ O ₃ (0.52–0.39–0.96) | 4.14×10^{-10} | 1723 |
| B [12] | Si | $(2.4 \pm 0.7) \times 10^{-8}$ | Melt state |
| Al [12] | Si | $(7.0 \pm 3.1) \times 10^{-8}$ | Melt state |
| P [12] | Si | $(5.1 \pm 1.7) \times 10^{-8}$ | Melt state |

Table 3 Experimental conditions and results for the CaO–SiO₂–CaCl₂ slag–silicon reaction at 1723 K

| No. | t/k_s | Weight of Si (g) | Weight of slag (g) | B content of Si (ppmw) | Change content of B in slag (ppmw) | Ratio of B removed to the gas phase (%) |
|-------|---------|------------------|--------------------|------------------------|------------------------------------|---|
| I-1 | 0 | 3.0 | 3.0 | 300 | 0 | 0 |
| I-2 | 0.3 | | | 233.5 | 20.7 | 15.3 |
| I-3 | 0.6 | | | 196.8 | 43 | 20.1 |
| I-4 | 0.9 | | | 136.4 | 51.8 | 37.3 |
| I-5 | 1.2 | | | 112.3 | 60.1 | 42.5 |
| I-6 | 1.5 | | | 85.7 | 54.5 | 53.3 |
| I-7 | 3.6 | | | 69.6 | 42.7 | 62.6 |
| I-8 | 7.2 | | | 68.1 | 40.3 | 63.9 |
| II-1 | 0 | 3.0 | 6.0 | 300 | 0 | 0 |
| II-2 | 0.3 | | | 225.0 | 14.37 | 15.4 |
| II-3 | 0.6 | | | 173.0 | 20.56 | 28.6 |
| II-4 | 0.9 | | | 126.0 | 33.59 | 35.6 |
| II-5 | 1.2 | | | 109.0 | 39.31 | 37.5 |
| II-6 | 1.5 | | | 83.7 | 44.15 | 42.7 |
| II-7 | 3.6 | | | 76.2 | 57.33 | 36.4 |
| II-8 | 7.2 | | | 65.4 | 38.89 | 52.3 |
| II-9 | 9 | | | 40.4 | 30.07 | 66.5 |
| II-10 | 12 | | | 40.3 | 30.35 | 66.3 |
| III-1 | 0 | 3.0 | 9.0 | 300 | 0 | 0 |
| III-2 | 0.3 | | | 217.6 | 24.5 | 3.0 |
| III-3 | 0.6 | | | 164.8 | 37.3 | 7.8 |
| III-4 | 0.9 | | | 122.7 | 40.7 | 18.4 |
| III-5 | 1.2 | | | 105.5 | 55.1 | 9.7 |
| III-6 | 1.5 | | | 70.3 | 57.2 | 19.4 |
| III-7 | 3.6 | | | 30.8 | 50.4 | 39.3 |
| III-8 | 7.2 | | | 31.6 | 49.2 | 40.3 |

In step (1) of the B-removal process, if it is assumed that the mass transfer of B in molten Si is very fast and that the distribution of B in molten Si is homogenous, then the condition $[B]_i = [B]_b$ is imposed. The diffusion coefficient of B in molten Si (D_{B-Si}) can therefore be found as $(2.4 \pm 0.7) \times 10^{-8}$ m/s² [12].

In step (2), the overall interfacial reaction of B removal can be represented by the following reaction:



Assuming this reaction occurs at the interface between molten Si and slag, and is in an equilibrium state, the reaction rate can be regarded as being very fast. This is predicated on the fact that Lei Zhang et al. [14] have reported that the mass transfer of boron oxide is the limiting control step in Na₂SiO₃–CaO–SiO₂ slag refining. However, if we assume instead that the chemical reaction is the rate-limiting step, then B transfer in both Si and slag is faster than the chemical reaction in the boundary layer due to the diffusion coefficients of B in both phases being of the same order. The distribution of B in the Si and slag should therefore exhibit a linear relation to distance; however, this is clearly reflected in the curve of the experimental results obtained. Thus, step (2) is not the rate-limiting step.

The process of step (3) is the transfer of B through the slag boundary layer adjacent to Si, as shown in Fig. 6. This means that the mass transfer of B in the slag, k_i , can be expressed as

$$J_3 = k_i (C_{B_i^{3+}} - C_{B_b^{3+}}) \quad (7)$$

In step (4), B is transferred through the slag boundary layer at the surface, and according to the definition of mass flux, the mass transfer coefficient of this process (k_s) can be expressed as

$$J_4 = k_s (C_{B_s^{3+}} - C_{B_b^{3+}}) \quad (8)$$

The change in the C_B of the bulk slag ($d(B^{3+})_b/dt$) has a relationship to $(J_3 - J_4)$, which is

$$\frac{dC_{(B^{3+})_b}}{dt} = \frac{S}{V_{\text{slag}}} (J_3 - J_4), \quad (9)$$

where S is the surface area and V_{slag} is the total volume of the bulk slag. By changing C_B to the weight percentage concentration of B (B^{3+}), and substituting Eqs. (7) and (8) into Eq. (9), we get

$$\frac{d(B^{3+})_b}{dt} = \frac{(J_3 - J_4)}{(V_{\text{slag}}/S)\rho_{\text{slag}}} = \frac{Sk_i}{m_{\text{slag}}} ((B^{3+})_i - (B^{3+})_b) - \frac{Sk_s}{m_{\text{slag}}} ((B^{3+})_b - \{B^{3+}\}_s), \quad (10)$$

where ρ_{slag} is the density, m_{slag} is the mass, and h is the height of the slag ($h = V_{\text{slag}}/S$). Considering the partition

Fig. 6 Profile of B transfer from molten Si to gas phase

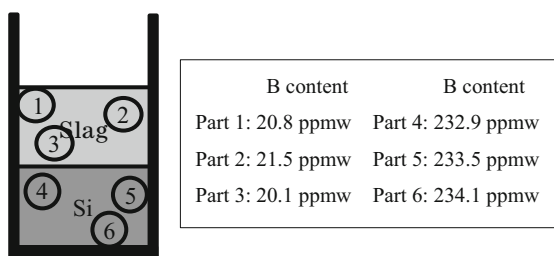
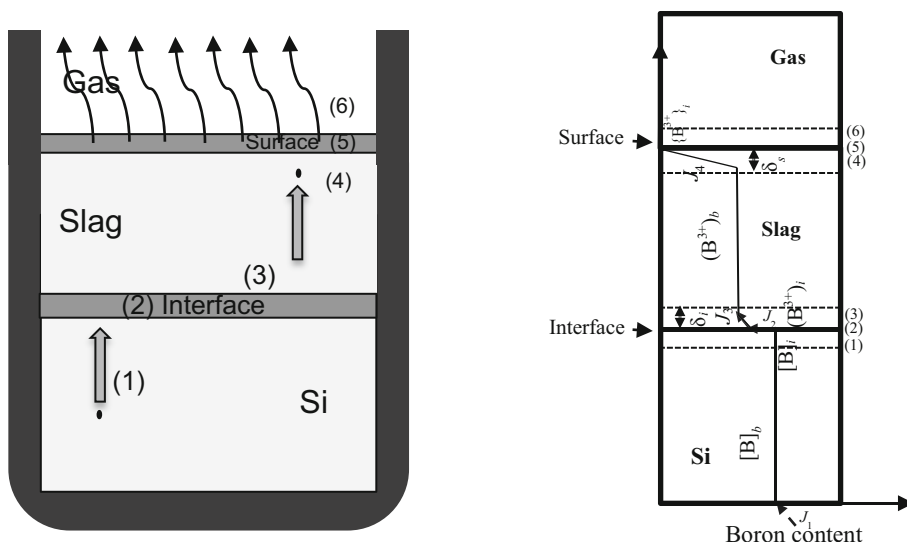


Fig. 7 Distribution of B in the slag and Si phase of sample I-2

ratio $L_B = (B)_i/[B]_i = (B)_e/[B]_e = 0.64$ [11] and $[B]_i = [B]_b$ of the chemical process, evaporation can be assumed to be so fast that the concentration of B at the surface, $(B^{3+})_s$, is zero. Thus, the equation can be simplified to

$$\frac{d(B^{3+})_b}{dt} = \frac{Sk_i}{m_{slag}} (L_B[B]_b - (B^{3+})_b) - \frac{Sk_s}{m_{slag}} (B^{3+})_b \quad (11)$$

In the same manner, J_1 can be assumed to be equal to the input flux of B into molten Si, which is zero. The value of J_2 is the flux of B in the interface between the Si and slag phases, as shown in Fig. 6, and therefore, the change in the C_B of the molten Si ($d[B]_b/dt$) has a relationship with $(J_1 - J_2)$ as

$$\frac{dC_{[B]_b}}{dt} = \frac{S}{V_{slag}} (J_1 - J_2) \quad (12)$$

According to the principle of mass conservation, the flux of B transferred from molten Si to the interface should equal the flux of B transferred from the interface to the slag bulk; which is to say, $J_2 = J_3$. Because $(B^{3+})_i = L_B[B]_b$ and $J_1 = 0$ in Eq. (12), we therefore get

$$\begin{aligned} -\frac{d[B]_b}{dt} &= \frac{J_3}{(V_{Si}/S)\rho_{Si}} = \frac{Sk_i}{m_{Si}} ((B)_i - (B^{3+})_b) \Rightarrow -\frac{d[B]_b}{dt} \\ &= \frac{Sk_i}{m_{Si}} (L_B[B]_b - (B^{3+})_b) \end{aligned} \quad (13)$$

Assuming $y = (B^{3+})_b$ and $x = [B]_b$, the first-order ordinary differential equation system for the mass transfer of B within bulk melts can be obtained from Eq. (11) and (13) as

$$\begin{cases} \frac{dy}{dt} = \frac{Sk_i L_B}{m_{slag}} x - \frac{S(k_i + k_s)}{m_{slag}} y \\ \frac{dx}{dt} = -\frac{SL_B k_i}{m_{Si}} x + \frac{Sk_i}{m_{Si}} y \end{cases}, \text{ when } t = 0, x = x_0, y = 0 \quad (14)$$

Solving Eq. (14) and assuming

$$\begin{cases} A = \left(-k_i - k_s - k_i L_B - \sqrt{-4k_i k_s L_B + (k_i + k_s + k_i L_B)^2} \right) / 2(m/S) \\ B = \left(-k_i - k_s - k_i L_B + \sqrt{-4k_i k_s L_B + (k_i + k_s + k_i L_B)^2} \right) / 2(m/S), \\ C = \sqrt{-4k_i k_s L_B + (k_i + k_s + k_i L_B)^2} \end{cases}$$

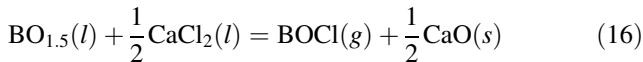
we get a general solution for x and y as

$$\begin{cases} x(t) = \frac{1}{2C} (-e^{At}k_i + e^{Bt}k_i - e^{At}k_s + e^{Bt}k_s + e^{At}k_iL_B \\ - e^{Bt}k_iL_B + e^{At}C + e^{Bt}C)x_0 \\ y(t) = -\frac{1}{C}(e^{At} - e^{Bt})k_iL_Bx_0 \end{cases}, \quad (15)$$

where $[B]_0 = 300$ ppmw, $\rho_{\text{slag}} = 2.01$ g/cm³, $\rho_{\text{Si}} = 2.57$ g/cm³, $S = 3.14$ cm², and $L_B = 0.64$. Because the initial content of B in the slag is 10.9 ppmw, the change in the B content of the slag is the difference between the actual content and 10.9 ppmw, as shown in Table 3. In Eq. (15), x and y are variables related to t , while k_i and k_s are the only unknown constants. Thus, k_i and k_s were obtained from the three sets of data displayed in Table 3 via a nonlinear regression analysis method using 1st Opt software. These results are shown in Fig. 8.

Figure 8 shows that the fitted values from the model for k_i (1.91×10^{-5} m/s) and k_s (2.50×10^{-5} m/s) are reasonable and agree with all three series results in the molten Si and slag, as is also shown in Table 4.

In step (5), the reaction between the slag and gas phase is assumed to occur at the surface in accordance with the following reaction [11, 15]:



As this means that the reaction rate is very rapid at high temperatures, step (5) is not the rate-limiting step. In the case of step (6), the diffusion of BOCl gas in an Ar atmosphere is likely to be very fast, and therefore, step (6) also cannot be the rate-limiting step.

The thickness of the boundary layers of slag adjacent to Si (δ_i) and at the surface (δ_s) can be calculated by

$$\delta_i = D_s/k_3 \delta_s = D_s/k_4 \quad (17)$$

Using (17), the different values of δ_i and δ_s for different mass ratios of slag and Si were calculated. As shown in Table 4, this found that the value of k_i (1.91×10^{-5} m/s) is slightly lower than that of k_s (2.50×10^{-5} m/s), which means that the rate-limiting step is controlled by both the boundary layer adjacent to Si and that at the surface. However, it is the former that has the greatest influence, because the thickness of the boundary layer of slag in the Si/slag interface (0.44 mm) is thicker than that at the surface (0.34 mm).

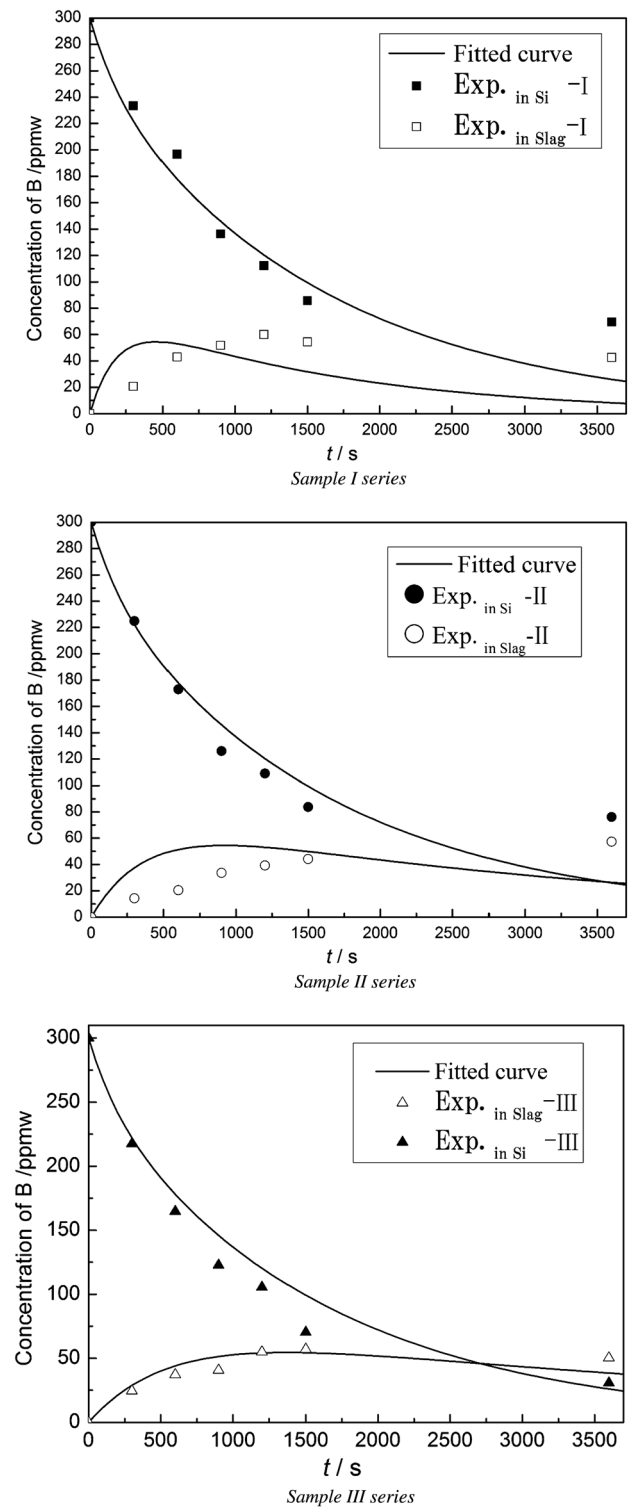


Fig. 8 Change in $(B^{3+})_b$ and $[B]_b$ with time

Table 4 k_i , k_s , δ_i , and δ_s with different mass ratios between slag and molten Si

| D_s (m ² /s) | k_i (m/s) | k_s (m/s) | δ_i (mm) | δ_s (mm) | Correlation coefficient |
|---------------------------|-----------------------|-----------------------|-----------------|-----------------|-------------------------|
| 8.46×10^{-9} | 1.91×10^{-5} | 2.50×10^{-5} | 0.44 | 0.34 | 0.97 |

Conclusion

To investigate the kinetics of the removal of B by evaporation using different compositions of CaO–SiO₂–CaCl₂ slags, a model for the transfer of B from Si to molten slag by diffusion and its evaporation as a gas phase was established. The mass transfer and diffusion coefficients of B in the slag were measured at 1723 K for different times and different mass ratios between the slag and Si. In addition, the rate controlling steps were also investigated based on the kinetics model and the calculated values of k_s and D_s . Thus, from this study, the following conclusions have been drawn.

- (1) The diffusion coefficient of B in slag (D_s) is 8.46×10^{-9} m²/s², which means the rate of step (3) is slower than that of B diffusion in Si [$(2.4 \pm 0.7) \times 10^{-8}$ m²/s²]. Thus, unlike other elements such as Al, Ca, Mg, and P, the rate-limiting step of B diffusion in CaO–SiO₂–CaCl₂ slag refining is controlled by the transfer of B in the slag.
- (2) With regards to the reaction rate, B oxidation (step 2), B oxychlorination (step 5), and the evaporation of BOC_l from the surface (step 6) all occur very quickly, and therefore, they cannot be considered rate-limiting steps. The mass transfer coefficient of B in slag was therefore measured and found to be 1.91×10^{-5} m/s for the transfer from the slag interface to the bulk slag, and 2.50×10^{-5} m/s for the transfer from the bulk slag to the surface.
- (3) The rate-limiting step in the removal of B from Si by slag refining is the transfer of B at both the boundary layer adjacent to Si and at the surface of the slag. However, the former of these has the greater influence, because the thickness of the Si/slag interface (0.44 mm) is greater than the boundary at the surface (0.34 mm).

References

1. Ma X, Yoshikawa T, Morita K (2013) Removal of boron from silicon-tin solvent by slag treatment. *Metall Mater Trans B* 44:528–533
2. Ma X, Yoshikawa T, Morita K (2013) Si growth by directional solidification of Si–Sn alloys to produce solar-grade Si. *J Cryst Growth* 377:192–196
3. Yuge N, Hanazawa K, Kato Y (2004) Removal of metal impurities in molten silicon by directional solidification with electron beam heating. *Metall Mater Trans B* 45:850–857
4. Martorano M, Neto JF, Oliveira T, Tsubaki T (2011) Macrosegregation of impurities in directionally solidified silicon. *Metall Mater Trans A* 42:1870–1886
5. Ma X, Yoshikawa T, Morita K (2012) Phase relations and thermodynamic property of boron in the silicon-tin melt at 1673K. *J Alloy Compd* 529:12–16
6. Li Y, Tan Y, Li J, Xu Q, Liu Y (2014) Effect of Sn content on microstructure and boron distribution in Si–Al alloy. *J Alloy Compd* 583:85–90
7. Suzuki K, Kumagai T, Sano N (1992) Removal of boron from metallurgical-grade silicon by applying the plasma treatment. *ISIJ Int* 32:630–634
8. Nakamura N, Baba H, Sakaguchi Y, Kato Y (2004) Boron removal in molten silicon by a steam-added plasma melting method. *Metall Mater Trans B* 45:858–864
9. Ikeda T, Maeda M (1992) Purification of metallurgical silicon for solar-grade silicon by electron beam button melting. *ISIJ Int* 32:635–642
10. Zheng S, Engh TA, Tangstad M, Luo XT (2011) Numerical simulation of phosphorus removal from silicon by induction vacuum refining. *Metall Mater Trans A* 42:2214–2225
11. Wang Y, Ma X, Morita K (2014) Evaporation removal of boron from metallurgical-grade silicon using CaO–CaCl₂–SiO₂ slag. *Metall Mater Trans B* 45:334–337
12. Kodera H (1963) Diffusion coefficients of impurities in silicon melt. *Jpn J Appl Phys* 2:212
13. Viswanathan LMNN, Seetharaman S (2012) Evaluating the chemical diffusion coefficient of sulfur in slag by metal analysis: model concept and experiments. 9th international conference on molten slags, fluxes and salts
14. Zhang L, Tan Y, Li J, Liu Y, Wang D (2013) Study of boron removal from molten silicon by slag refining under atmosphere. *Mater Sci Semicond Process* 16(6):1645–1649
15. Bjerke H (2012) Removal of boron from silicon by slag treatment and by evaporation of boron from slag in hydrogen atmosphere. Doctoral dissertation, Norwegian University of Science and Technology, p 35